

Mirror displacement energies and neutron skins.

J. Duflo^a, and A. P. Zuker^b

(a) Centre de Spectrométrie Nucléaire et de Spectrométrie de Masse (IN2P3-CNRS) 91405 Orsay Campus, France
 (b) IReS, Bât27, IN2P3-CNRS/Université Louis Pasteur BP 28, F-67037 Strasbourg Cedex 2, France

(Dated: February 9, 2020)

Assuming isospin conservation, it is shown that a single expression accounts for both neutron and proton radii. Excellent fits to the former turn out to be consistent with different neutron skins. To fix their values the displacement energies between mirror nuclei, MDE, are calculated using an accurately derived Coulomb energy, and smooth averages of the charge symmetry breaking potentials constrained to state of the art values. Optimum agreement with observed MDE and neutron skins is obtained. The remaining uncertainties are shown to be due to shell effects.

PACS numbers: 21.10.Sf, 21.10.Ft, 21.10.Gv, 21.60.Cs

Recent experiments [1, 2] have considerably added to our knowledge of neutron radii, the most elusive of the fundamental properties of nuclear ground states. The two sets of measures are consistent with one another, and a recognizable pattern emerges [1, Fig. 4], leading to an estimate for the neutron skin ($\nu \equiv$ neutrons, $\pi \equiv$ protons, $t = N - Z$)

$$\Delta_{r_{\nu\pi}} = \sqrt{\langle r_{\nu}^2 \rangle} - \sqrt{\langle r_{\pi}^2 \rangle} = -0.04(3) + 1.01(15) \frac{t}{A} \text{ fm. (1)}$$

A third—totally different—experiment [3] adds enormous weight to this estimate: it deals with the sodium isotopes, lighter and far more exotic than the species studied in [1, 2]. Nonetheless, their $\Delta_{r_{\nu\pi}}$ behaviour is very much the same, as seen in Fig. 1.

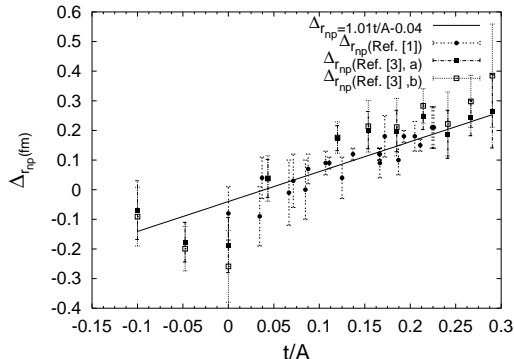


FIG. 1: $\Delta_{r_{\nu\pi}}$ from: [1, Fig. 4] (circles), the two approximations of Ref. [3, Table I] (squares), and Eq. (1)

On the theory side, we have an elegant analysis of $\Delta_{r_{\nu\pi}}$ [4], and many mean-field calculations. Some of them do very well, others not so well [5], though in the Na isotopes several Skyrme forces seem to give equally good results [6]. As was pointed out in [7], the neutron skin could be easily varied in such forces, without perturbing other observables, but the criteria to fix it were not obvious. The problem has been tackled head on recently [8, 9] by constraining agreement with realistic calculations of the equation of state for neutron matter.

There is—in principle—a very precise alternative experimental source of neutron radii: proton radii. This statement may seem surprising, but it is very easy to prove. After proposing an epitome of its consequences we shall proceed to the full version.

First note that isospin conservation implies that *once we know the proton radius for the ($Z N$) nucleus we know the neutron radius for its mirror where Z and N are interchanged*. Though we seldom know the square radius $\langle r_{\pi}^2 \rangle$ for $Z > N$, by using the isospin properties of the r^2 operator, an expression for $\langle r_{\pi}^2 \rangle$ can be derived that gives automatically the value of $\langle r_{\nu}^2 \rangle$: Eq. (2) will be shown to rest on exactly the same arguments that lead to the famous isobaric multiplet mass equation (IMME).

In practice, we shall find that—upon fitting $\langle r_{\pi}^2 \rangle$ to the wealth of available data—very good agreement can be obtained for a wide range of neutron radii.

To filter the candidates we shall resort to the energy displacements between mirror states, MDE, a term we prefer to the usual CDE (Coulomb displacement energies) because in addition to the Coulomb force, the nuclear charge symmetry breaking (CSB) potential is involved.

The method is based on the reduction of all quantities to expressions that depend only on A and t (or N and Z), which we shall call BeWe as an homage to the Bethe Weizsäcker mass formula. However the reduction will involve only averages over *microscopic* quantities without relying on semiclassical arguments. In the process, shell effects are ignored. They will show as deviations between calculated and observed MDE leading to a limit of ≈ 200 keV for optimal agreement. Our work amounts to data analysis based on three expressions:

Eq. (2) for the radii, already mentioned, only assumes isospin conservation.

In Eq. (6), V_B is a BeWe form for a CSB interaction, constrained to agree with state of the art estimates [10]. The auxiliary term V_A contains the only free parameter in the calculations. Its role is non-essential but indicative of the magnitude off effects not accounted for explicitly.

Eq. (10) for the Coulomb contribution is a rigorous

result that will be carefully derived.

The calculations will spontaneously select neutron skins compatible with expression (1) and optimal MDE. Therefore we obtain simultaneously good radii, good MDE, and realistic CSB parameters. The present status of an old problem, the Nolen Schiffer (NS) anomaly—historically associated to systematic deviations from the observed MDE when rigorous estimates are carried out [11]—will be seen to reduce to the explanation of (smooth) shell effects.

The first task is to exhibit the isospin structure of the proton square radius operator. From the equality

$4r_\pi^2 = (r_\pi + r_\nu)^2 + (r_\pi - r_\nu)^2 + 2(r_\pi + r_\nu)(r_\pi - r_\nu)$ it follows that it is a sum of isoscalar, isotensor and isovector terms. Using Wigner Eckart theorem, their expectation values between states of good T, T_z will yield contributions that go as 1, $3T_z^2 - T(T+1) \equiv \hat{t}^2/2$, and T_z , respectively. As only ground states with $T = |t|/2, T_z = t/2$ are accessible, $\hat{t}^2 \approx t^2$, and—neglecting terms in $(t/A)^3$ and higher—we can write the radius as

$$\rho_\pi = \sqrt{\langle r_\pi^2 \rangle} = A^{1/3} \left(\rho_0 - \frac{\zeta}{2} \frac{t}{A^p} - \frac{v}{2} \left(\frac{\hat{t}}{A} \right)^2 \right) e^{(g/A)}, \quad (2)$$

and a similar expression for ρ_ν with $t \Rightarrow -t$. The $e^{(g/A)}$ term reflects the larger radii for small A . The exponential form stresses that the coefficients ρ_0, v and ζ in Eq. (2)—though they will be treated as constants—are, in principle, functions of A and T . Clearly $v > 0$ represents a uniform contraction of the fluids, while $\zeta > 0$ implies a π -contraction and ν -dilation. The terms in v and ζ must be *at most* of the same order as ρ_0 for large t/A and the only remaining uncertainty is in the scaling p in t/A^p , which gives the neutron skin

$$\Delta_{r_{\pi\nu}} \equiv \Delta(\zeta) = (\rho_\nu - \rho_\pi) = \frac{\zeta t}{A^{p-1/3}} e^{(g/A)}. \quad (3)$$

If $p = 1$ the volumes occupied by the two fluids may differ by a quantity of order A , and we have a “volume” skin.

If $p = 4/3$ we have a “surface” skin, since the difference in volumes is at most of order $A^{2/3}$.

The volume option would be the correct one for strong attraction between like particles. In nuclei, the $\nu\pi$ force is by far the strongest, and we expect a surface skin.

To determine the coefficients in Eq. (2) we shall fit to 634 experimental values of charge radii (full references are given in [12]), reduced to point radii through the standard prescription $\rho_\pi^{exp} = [\langle r_\pi^2 \rangle_{charge}^{exp} - 0.64]^{1/2}$. We proceed in two steps.

First we fit 82 experimental values for nuclei with N or $Z = 6, 14, 28, 50, 82, 126$ (the EI closures defined below), for which shell effects can be assumed to be minimal. The results are altogether remarkable: for $0.4 \leq \zeta \leq 1.2$ the root mean square deviations (rmsd) are below 10 mf. The corresponding values of v are given

in Table I for $0.6 \leq \zeta \leq 1$. For the other parameters we find $\rho_0 = 0.943(2)$, $g = 1.04(3)$.

Then, to check the stability of these numbers, we keep them fixed and fit a shell corrected radius

$$\rho_\pi^{sc} = \rho_\pi + \mathcal{D}, \quad \mathcal{D} = \lambda S_\pi S_\nu + \mu Q_\pi Q_\nu.$$

The correction \mathcal{D} acts in the EI (extruder-intruder) valence spaces consisting in the orbits of harmonic oscillator shell p , except the largest (extruder), plus the largest (intruder) orbit from shell $p+1$. For protons, say, the EI degeneracy is $D_\pi = (p_\pi + 1)(p_\pi + 2) + 2$ (e.g., $p_\pi = 3$ between $Z = 28$ and $Z = 50$). The degeneracy of the non intruder orbits is $D_{r\pi} = p_\pi(p_\pi + 1)$. Now call z the number of valence protons, and define $S_\pi = z(D_\pi - z)/D_\pi^2$, $Q_\pi = z(D_{r\pi} - z)/D_\pi^2$; and similarly for neutrons. By construction, \mathcal{D} vanishes at the EI closures.

The results are again remarkable: with $\lambda = 5.6(2)$, $\mu = 23(1)$ we obtain $\text{rmsd} \leq 11$ mf in all cases. Fig. 2 gives an idea of the quality of the fits: most of the calculated points fall within (or very close to) the experimental error bars. The exceptions are the light nuclei and the region around the light P_t isotopes, both known for their complex radial behavior. A volume skin also leads to excellent radii, but it will be ruled out by the MDE.

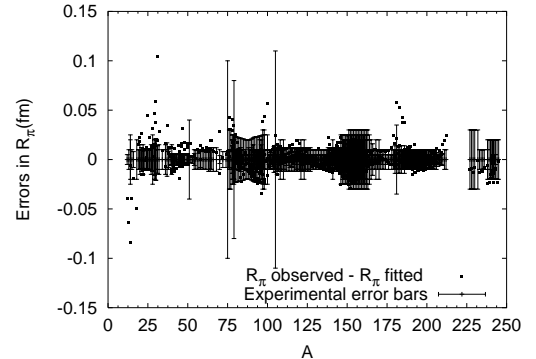


FIG. 2: Comparison of experimental and calculated errors for $R_\pi = (5/3)^{1/2} \rho_\pi$ ($\zeta = 0.8$, undistinguishable from other choices.)

It should be stressed that these excellent fits must be viewed as a *fringe benefit*: The \mathcal{D} corrections will be ignored from now on. They were only introduced to confirm the consistency of the possible ζ, v pairs which affect the Coulomb energies through their dependence on ρ_π , which we establish next.

The oscillator basis provides the natural quantization condition in a many body context, i.e., in Fock space. The frequency $\hbar\omega$ will be calculated as in [13, Eq. (2-157)], but here we introduce a refinement, by treating separately neutrons and protons:

$$\frac{\hbar\omega_\pi}{(2Z)^{1/3}} = \frac{35.59}{\langle r_\pi^2 \rangle} \approx \frac{\hbar\omega_\nu}{(2n)^{1/3}} \approx \frac{\hbar\omega}{(A)^{1/3}}, \quad (4)$$

where the approximations hold only for $\langle r_\pi^2 \rangle \approx \langle r_\nu^2 \rangle$. To make contact with standard use, we write the Coulomb

potential V_C in terms of the equivalent radius $R_\pi = (5/3)^{1/2}\rho_\pi$. Calling upon Eq. (4) we have

$$V_C = e^2 \sqrt{\frac{M\omega_\pi}{\hbar}} \widehat{\left(\frac{1}{r}\right)} = \frac{1.934}{R_\pi} Z^{1/6} \widehat{\left(\frac{1}{r}\right)}, \quad (5)$$

where $\widehat{(1/r)}$ is a two body operator that will be dealt with in detail later.

For the charge symmetry breaking (CSB) terms we write directly their BeWe expressions.

$$V_B = -\frac{1}{2} \left(B_v t - B_s \frac{t}{A^{1/3}} \right), \quad V_A = -A_t \frac{t^3}{A^{4/3}}. \quad (6)$$

The parameters B_v and B_s *cannot* be chosen arbitrarily. They are not known experimentally, but enormous theoretical work has been devoted to CSB potentials, extensively described in Ref. [10], from which we take the V_B contribution to be ≈ 100 keV at $A = 17$, and ≈ 300 keV in nuclear matter. Accordingly, we define a standard V_B^{st} at $B_v = 300$ keV and $B_s = 500$ keV. Note that neutrons are more bound, so V_B always gives a positive contribution to MDE=BE($Z_>, N_<$)-BE($Z_<, N_>$).

The V_A term stands for all effects not accounted for by $V_B + V_C$. They are assumed to be perturbative (at least a factor t/A smaller than V_B) but their precise form is irrelevant ($t|t|/A$ or t^3/A^2 have practically the same effects). To all their possible origins (see [15] for a list), we may add one that seems to have been overlooked: Even in the absence of V_C , a mean field calculation *always* violates T -conservation when forcing $\omega_\pi \neq \omega_\nu$. Therefore, projection to good T is necessary (and probably significant) in the conserving approximation we are using.

Table I compares 78 experimental MDE, extracted from [14], with calculated ones. The first column in bold-face gives the rmsd when only $\langle V_{Cm}^d \rangle$ from Eq. (10) is included. The preferred value at $\zeta \leq 0.7$ moves to $\zeta = 0.8$ -0.9 for $V_C + V_B^{st} \equiv V_{C+B}^{st}$, and *stays close* at $\zeta = 0.7$ -0.8 when A_t is allowed to vary: though V_A may represent genuine effects, it affects ζ very little. Finally B_v , B_s and A_t are allowed to vary simultaneously to give an idea of the range of plausible V_B parameters. Note that $B_v - 0.4B_s$ gives the contribution at $A \approx 16$. Allowing for uncertainties we propose $\Delta_{r_\nu\pi} = 0.8(1) t/A$, compatible with Eq. (1).

The next task is to derive Eq. (10). Following Ref. [16] we separate the Hamiltonian $H = H_m + H_M$. The monopole part H_m contains all terms in scalar products of fermion operators ($a_r^+ \cdot a_s$) for sub-shells r and s , and is responsible for spherical Hartree Fock variation. Here we consider only the *diagonal* terms involving the number operators $m_r = a_r^+ \cdot a_r$. The multipole H_M only contributes to shell effects [16, 17, 18]. Calling $V_{ikik'}$ the matrix elements of $\widehat{\frac{1}{r}}$, the diagonal monopole part is

$$\widehat{\left(\frac{1}{r}\right)}_m^d = \sum_{i \leq k} \frac{z_i(z_k - \delta_{ik})}{1 + \delta_{ik}} V_{ik}, \quad V_{ik} = \frac{\sum_J V_{ikik}^J[J]}{\sum_J [J]}, \quad (7)$$

TABLE I: Root mean square deviations from observed MDE for three sets of coefficients in Eq. (6). V_C from Eq. (10). All energies in keV. See text.

ζ	v	V_C	V_{C+B}^{st}	$V_{C+B}^{st} + V_A$		$V_C + V_B + V_A$			rmsd
		rmsd	rmsd	A_t	rmsd	B_v	$.4B_s$	A_t	
1.0	0.51	512	294	032	287	549	349	136	181
0.9	0.57	421	257	079	222	435	271	146	180
0.8	0.62	335	269	129	182	306	182	157	179
0.7	0.68	282	334	181	191	177	093	169	178
0.6	0.73	281	428	233	248	047	003	181	178

$[J] = 2J + 1$, z_k = number of protons in orbit k , where $k \equiv plj$ stands for the quantum numbers specifying a given harmonic oscillator (ho) orbit (p is the principal quantum number). Following [16], the sum over the first κ major shells containing τ orbits is reduced to a sum of factorable terms by diagonalizing the matrix $\frac{1}{2}\{V_{ik}\}$ through the unitary transformation \mathcal{U} :

$$\widehat{\left(\frac{1}{r}\right)}_m^d = \frac{1}{2} \left[\sum_n \mathcal{E}_n \left(\sum_k z_k \mathcal{U}_{kn} \right)^2 - \sum_k z_k V_{kk} \right], \quad (8)$$

By rescaling $\mathcal{E}_n = \tau E_n$, $\mathcal{U}_{kn} = (\tau)^{-1/2} U_{kn}$, the results become independent of τ . For $\kappa = 8$, $\tau = 36$ the diagonalization produces a largest eigenvalue $E_\tau = 0.383$ that is 30 times larger than the next and over 100 times larger than the second next. Increasing κ only increases the number of negligible terms: The leading one amounts to a basically exact representation in Fock space. Within a major shell p we have to good approximation $U_k \equiv U_{k\tau} = U_p - 0.01 L^2/(p + 3/2)$, where $L^2 = l(l+1) - p(p+3)/2$ (i.e., $l(l+1)$ referred to its centroid), while the average over j orbits is—to leading order in a $(p+1)^{-\alpha}$ expansion— $U_p \approx 1.52(p+1)^{-1/4}$. For $V_k \equiv V_{kk}$ the equivalent result is $V_p \approx 0.93(p+3/2)^{-1/2}$, but the j -dependence is more complicated.

In keeping with our policy of extracting smooth BeWe forms, we average over sub-shell occupancies by setting $U_k = U_p$, replacing $z_k \equiv (p+1)(p+2) = D_p$, and treating p as a continuous variable. Then, the leading term in Eq. (8) becomes (numerically, with $\approx .1\%$ accuracy)

$$\begin{aligned} \langle \widehat{\left(\frac{1}{r}\right)}_m^d \rangle &\approx \frac{1}{2} \left[E_\tau \langle \sum_p D_p U_p \rangle^2 - \langle \sum_p D_p V_p \rangle \right] \quad (9) \\ &\approx 0.444 \left[(Z - 1/2)^{2-1/6} - Z^{1.006-1/6} \right], \end{aligned}$$

which inserted in Eq. (5) yields (in round numbers and obvious notation)

$$\langle V_{Cm}^d \rangle \approx \frac{.858 Z^{1/6} [(Z - 1/2)^{2-1/6} - Z^{1-1/6}]}{R_\pi} \quad (10)$$

$$\approx \frac{.864 (Z(Z - 1) - Z)}{R_\pi^c}. \quad (11)$$

In Eq. (11) we have replaced the point radius parameter $R_0 = \sqrt{5/3}\rho_0 = 1.219$ by its charged value $R_0^c = 1.226$, and changed accordingly the overall coefficient, which becomes the one for the classical charged sphere: $\langle V_{Cm} \rangle = 3e^2 Z^2 / 5R^c \approx 0.864 Z^2 / R^c \approx 0.7 Z^2 / A^{1/3}$. A truly satisfactory result illustrating the power and flexibility of the factorable representations in Fock space.

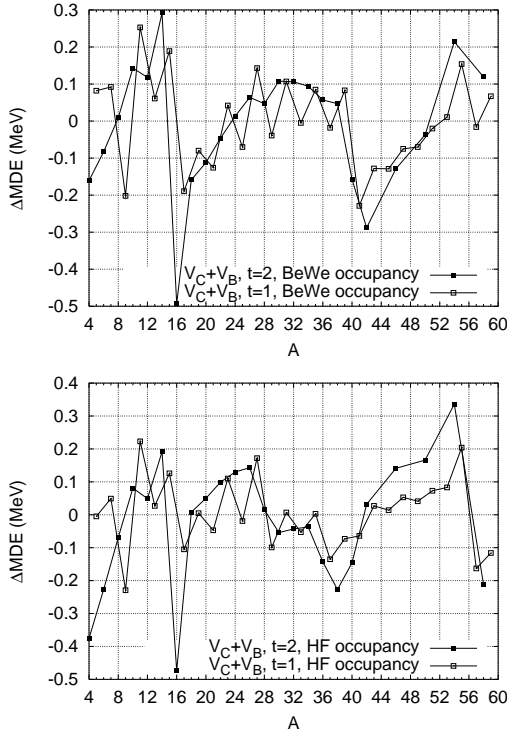


FIG. 3: First panel: Experimental–calculated MDE for $t = 1$ and 2 with smooth BeWe occupancies ($\zeta = 0.8$). Second panel: As above for Hartree Fock occupancies.

The form of averaging we have used eliminates all shell effects, which show cleanly in the first panel of Fig. 3 as the difference between experimental and calculated values. For clarity only $t = 1$ and 2 cases are kept. They are sufficient to indicate the secular nature of the deviations, which will provide useful hints when the time of a full description comes.

The alternative to smooth filling is *ordely* filling. The calculation now demands we use the exact values for U_k and V_k in the leading term of Eq. (8). The result is very close to that of a Hartree Fock (HF) variation, since Coulomb matrix elements are rather unsensitive to details of the single particle wavefunctions, except in the case of halo orbits. Examination of the deviations for the HF filling in the second panel of Fig. 3 reveals a dramatic improvement for the $A = 15-17$ and $A = 39-41$ pairs, the two test cases most extensively studied in the literature ([10, 11, 15] and references therein). This gain is upset by a loss of regularity in the shell-effect patterns and the (apparent) need for a too strong V_B . If we keep V_B^{st} (and

$\zeta = 0.8$) at 330 KeV the rmsd becomes large. To reduce it, in the figure we have allowed $B_v - 0.4B_s = 500 - 250$ KeV, leading to rmsd=194 keV. This result is in line with the findings of Ref. [19], where a good HF description of the MDE with the SKXcsb force is achieved with a V_B contribution of 355 keV at $A = 17$.

These numbers and the patterns in Fig. 3 indicate that shell effects—of monopole (HF) and multipole origin—should be treated together.

To sum up: We have proposed a method based on smooth BeWe expressions—including a very precise form of the Coulomb energy—that establishes the compatibility of observed nucleon radii and MDE with state of the art CSB potentials. The only free parameter turns out to be useful but not essential. Its meaning will become clear once we learn how to deal with the shell effects that appear to have some systematic behaviour in which is hidden what remains of the NS anomaly. Hence the intriguing question: what is the interplay of Coulomb and CSB potentials in the shell effects?

We thank J. Bartel for his patient coaching on Skyrme calculations, G. Martínez for his help, and R. Machleidt, M. Horth-Jensen and P. Vogel for their comments.

- [1] A. Trzcínska *et al.*, Phys. Rev. Lett. **87**, 082501 (2001).
- [2] A. Krasznahorkay *et al.*, Phys. Rev. Lett. **82**, 3216 (1999).
- [3] T. Suzuki *et al.*, Phys. Rev. Lett. **75**, 3241 (1995).
- [4] C. J. Pethick and D. G. Ravenhall, Nucl. Phys. **A606**, 173 (1996).
- [5] J. Dobaczewski, W. Nazarewicz, and T. Werner, Z. Phys A **354**, 27 (1996).
- [6] B. A. Brown and W. A. Richter, Phys. Rev. C **54**, 673 (1996).
- [7] J. M. Gómez and J. Martorell, Nucl. Phys. **A410**, 475 (1983).
- [8] E. Chabanat, P. Bonche, P. Haensel, J. Meyer and R. Schaeffer, Nucl. Phys. **A627**, 710 (1997).
- [9] B. A. Brown, Phys. Rev. Lett. **85**, 5296 (2000).
- [10] R. Machleidt and H. Müther Phys. Rev. C **63**, 034005 (2001).
- [11] J. A. Nolen and J. P. Schiffer, Ann. Rev. Nuc. Sci. **19**, 471 (1969).
- [12] J. Duflo, Nucl. Phys. **A576**, 29 (1994).
- [13] A. Bohr and B. Mottelson, *Nuclear Structure* vol I (Benjamin, Reading, 1964).
- [14] G. Audi and A.H. Wapstra, Nucl. Phys. **A595**, 409 (1995).
- [15] B. K. Agrawal, T. Sil, S. K. Samaddar, J. N. Dee, and S Shlomo, Phys. Rev. C **64**, 024305 (2001).
- [16] M. Dufour and A. P. Zuker, Phys. Rev. C **54**, 1641 (1996).
- [17] A. P. Zuker, Nucl. Phys. **A576**, 65 (1994).
- [18] J. Duflo and A. P. Zuker, Phys. Rev. C **59**, R2347 (1999).
- [19] B. A. Brown, W. A. Richter, and R. Lindsay, Phys. Lett. B **483**, 49 (2000).